Journal of Orthopaedic Research
15:437-441 The Journal of Bone and Joint Surgery, Inc.

Small-Angle HeNe Laser Light Scatter and the Compressive Modulus of Articular Cartilage

Ian S. Kovach and Kyriacos A. Athanasiou

Biomechanics Laboratory, Department of Orthopaedics, University of Texas Health Science Center, San Antonio, Texas, U.S.A.

Summary: Light scattering is a widely used technique for probing the microarchitecture and interactions of biological materials and solutions. In this paper, we describe the use of this method in the study of articular cartilage. The experiments presented utilize small-angle static scattering of HeNe laser light (632.8 nm) from 40 μm thick samples of cartilage taken from the superficial zone of baboon femoral condyle. The specimens were taken from a total of 26 sites in eight animals of various ages. In addition to measuring the dependence of the intensity of scattered light on scatter angle, we performed mechanical testing at the test sites using creep-indentation techniques. The results from the optical and mechanical experiments were compared, and a significant correlation was noted between the average scatter angle and the compressive aggregate modulus. In addition, it was noted that the cartilage of skeletally immature animals had a smaller aggregate modulus and scattered to a higher average angle than the cartilage of skeletally mature animals. A quantitative theory was developed to explain the relation between mechanical and optical properties in terms of the degree of order in the spatial arrangement of the collagen fibers in cartilage.

By studying the scattering of light from a material or solution, it is possible to characterize aspects of both its structure and internal interactions. Variations on this technique are widely used and have made significant contributions to the understanding of a variety of macromolecular solutions, including micelles (4), protein solutions (3), proteoglycan in solution (14), and various synthetic polymers. Light-scattering techniques have also been used to study the architecture of collagen fibers in dermis (8) and tendon (15). In addition, the physical basis for the transparency of the cornea has been explained in terms of scattering from the ordered collagen fiber matrix (2). The results of these studies indicate that light scattering can be used to characterize the arrangement of collagen fibers in biologic tissues.

To our knowledge, light-scattering techniques have not been used to study articular cartilage. As a material, cartilage seems particularly well suited to the use of these techniques. Cartilage has several important structural features whose size scales are near the wavelength of visible light. Collagen fiber diameter, interfiber distance, and proteoglycan aggrecan size are all within an order of magnitude of typical optical wavelengths (5,12).

It is our hypothesis that the microarchitecture, as determined by light-scattering techniques, is directly related to the mechanical properties and age of the specimen. To assess these relationships, mechanical testing and static small-angle light-scattering experiments were performed on thin-sliced specimens of cartilage taken from the femoral condyle of a baboon. The average scatter angle was measured and was compared with the compressive mechanical properties as determined by creep-indentation experiments. A semi-empirical theory was then developed in an attempt to explain the observed results in terms of collagen fiber arrangements.

METHODS

Experimental Methodology

A total of 26 sites from eight left femoral condyles taken from baboons of various ages were examined using creep-indentation experiments and small-angle light scattering. The samples were from predetermined sites on the condyles (Fig. 1). Four sites were designated for each knee; however, six samples were not usable for light scattering due to difficulties with slicing. A larger series examining the compressive properties of distal femoral cartilage in this species demonstrated no statistically significant site-dependent variation in the mechanical properties among these test sites (13). Three animals (nine sites) were skeletally immature, and five animals (17 sites) were skeletally mature. Skeletal maturity was defined as 3 years old or older.

The creep-indentation experiments were performed by indent-

Received April 11, 1996; accepted January 22, 1997.
Address correspondence and reprint requests to I. S. Kovach at Biomechanics Laboratory, Department of Orthopaedics, University of Texas Health Science Center, 7703 Floyd Curl Drive, San Antonio, TX 78284-7774, U.S.A.

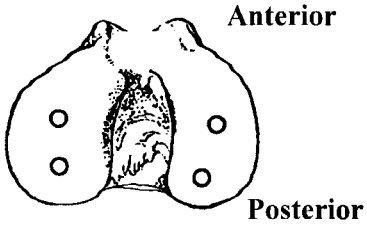

FIG. 1. Location of test sites from the distal femora of baboons.

ing full-thickness cartilage samples still attached to bone, prior to their preparation for scattering, with a computer-controlled porous probe. In this technique, a step load of 0.084 N is applied perpendicularly, under computer control, to the articular surface through a 1 mm diameter porous probe until creep equilibrium is achieved. The displacement and force are recorded as functions of time and analyzed using a finite element model of the biphasic theory (9) to yield the aggregate modulus, permeability, and Poisson's ratio at the test sites. The thickness of the samples was determined in skeletally mature animals by mounting a needle on the force-transducing probe, penetrating the cartilage at fixed velocity, and observing the location of force changes that correspond to entering the cartilage and the subchondral bone. In the case of immature specimens, the thickness of the cartilage was determined on the basis of the microscopic examination. Details regarding the instrumentation, method of mechanical data analysis, and determination of thickness were previously published (1).

After being mechanically tested, the specimens were refrozen until preparation for the scattering experiments. The samples were subjected to a total of three freeze-thaw cycles following dissection: the first, prior to mechanical testing; the second, between mechanical testing and sample preparation for light scattering; and the third, during thin-slicing with the cryostat.

The cartilage samples for scattering were taken from the mechanical test sites at a fixed depth from the surface (60 μm). A cryostat was used first to remove the most superficial 60 μm of the cartilage, parallel to the articular surface. A 40 μm thick slice was then obtained using the cryostat and was wet-mounted on a glass slide for scattering. The average thickness of the entire cartilage at the sites tested was 2.23 ± 1.49 mm. This corresponds to taking the scatter samples from an average of 2.7% (range: 1.6-8.1%) of the total thickness from the surface. The superficial zone of cartilage is composed of the outermost 10-20% (11), and accordingly the scatter samples were taken from this zone.

The light-scattering experiments were performed with a polarized 1 mW HeNe laser (model 1508-8; Uniphase, San Jose, CA, U.S.A.) at 632.8 nm. A digital camera (model XC75; Sony, Tokyo, Japan) was used for data acquisition. The laser beam was attenuated using neutral density filters to prevent detector saturation, with a resultant beam power of approximately 10 μW. The lens was removed from the camera, and the scatter was directed onto the digital chip that was placed 1.5 cm from the sample (Fig. 2). The resulting digitized image was acquired and processed using the NIH Image software package (National Institutes of Health, Bethesda, MD, U.S.A.) on a Macintosh computer. The intensity profile of the incident beam was acquired and was subtracted from the sample scatter pattern to yield the scatter intensity.

The average scatter angle was then determined by converting pixels into degrees, on the basis of the setup geometry. The average scatter angle was calculated by weighting the angle with the intensity, i.e.,

$$\langle\theta\rangle = I_{tot}^{-1} \int \theta I(\theta) d\Omega \qquad (1)$$

where $\langle\theta\rangle$ is the average scatter angle, θ is the azimuthal angle from the beam axis, I is the intensity of scatter, I_{tot} is the total scatter intensity, and $d\Omega$ is a solid angle element. This average was approximated by calculating the average angle as determined along eight evenly spaced rays extending out from the center of the scatter pattern for each image.

Analytical Methodology

The scatter intensity, as a function of angle, is the product of the angular dependence of the scatter from a single element and the Fourier transform of the fluctuations in the density-density correlation function of scattering elements (6):

$$I(\theta) = M(\theta)\, S(\theta) \qquad (2)$$

where M is the angular dependence of scatter from an individual scattering element. S is sometimes called the structure factor and is defined as

$$S(\vec{k}) = \int d^3\vec{r} e^{i(\vec{k}\cdot\vec{r})} \langle\rho(\vec{r})\rho(\vec{0})\rangle \qquad (3)$$

where $\langle\rho(\vec{r})\rho(\vec{0})\rangle$ is the fluctuation in the density-density correlation function; $\vec{k}$, the momentum transfer, is related to θ by, $|\vec{k}| = 4\pi\lambda^{-1} \sin(\theta/2)$, where λ is the wavelength of the scattered light. The integral in Eq. 3 is taken over the scatter volume.

In the case of long rods, such as collagen, the scatter pattern from individual rods can be solved both analytically and computationally (2,18). The small-angle scatter technique takes advantage of a window of relatively constant values of M at highly forward scatter. In this case, variations in the scatter resulting from changes in the structure factor can be seen without the large dynamic range required at higher angles.

It is illustrative to consider qualitative features of the radial density-density correlation function and their resulting effects on the small-angle scatter pattern. The density-density correlation function is the probability of finding a second scattering element at a location given that a scattering element is located at the origin of the coordinate system. A model correlation function will have a value of 0 at the origin (scattering elements cannot occupy the same location) and will have a decaying periodic structure with increasing distance. A reasonable trial function for the fluctuations in the radial density-density correlation function can be approximated by

$$\langle\rho(\vec{r})\rho(\vec{0})\rangle = \rho_0 e^{-r/\xi} \cos(r/r_0) \qquad (4)$$

where ρ_0 is the average density, ξ is the spatial correlation length or short-range order parameter, and r_0 is the average spacing between scattering elements (2).

The periodicity in Eq. 4 reflects the presence of interactions, and its spatial frequency results from the average spacing between scattering elements. The decay in the fluctuations represents the fact that whatever interactions exist are short range and thus are "forgotten" beyond a certain distance, related to ξ. Beyond a certain distance, the correlation function has decayed to the average likelihood of finding a second scattering element.

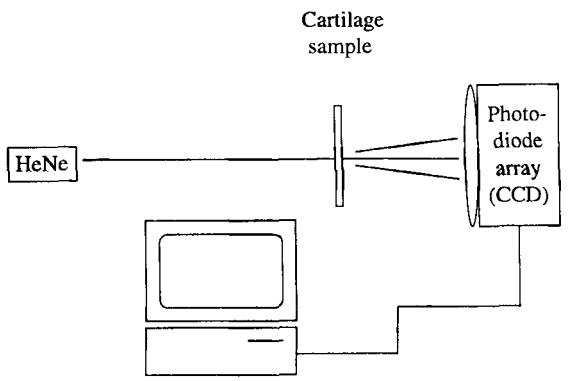

FIG. 2. Experimental setup. CCD = digital camera.

The implications of these qualitative features of the density-density correlation function provide significant insight into the small-angle scatter pattern. By Fourier transforming the trial correlation function to determine its manifestation in the small-angle scatter pattern, some interesting features are immediately evident. In addition to the peak associated with the periodicity of the correlation function (at relatively large angles), there is a second peak centered on $\theta = 0$ whose width is inversely related to ξ:

$$\langle\theta\rangle \approx \frac{\lambda}{\xi} \tag{5}$$

where ξ, θ, and λ are as previously defined.

The short-range order parameter is directly manifest in the small-angle scatter width or average scatter angle. The spatial frequency corresponding to the average spacing of collagen fibers gives rise to scatter at much higher angles, i.e., 40°, whereas the widths of the small-angle scatter observed in our experiments correlate to short-range order over approximately 8 μm. This degree of short-range order is qualitatively consistent with electron microscopy studies of articular cartilage (10), although quantitative determinations of collagen fiber arrangement were not undertaken in those studies.

Thus, the results for width of the average scatter angle, as determined in these experiments, can provide a measure of the degree of short-range order within the collagen fiber network. This parameter must be intimately related to collagen fiber interactions, which in turn would be expected to be manifest in the mechanical properties of the cartilage. The observed relationship between the compressive mechanical properties of cartilage and its small-angle light scattering can be explained theoretically in a semi-empirical manner.

To understand the results demonstrated in Fig. 3, it is necessary to introduce a parameter, n, that characterizes the degree of collagen fiber interaction. Because the nature of collagen fiber interaction in cartilage is not completely understood, the exact meaning of n is kept general, i.e., as n increases, the degree of collagen fiber interaction increases. This allows for both direct interfiber interactions such as crosslinks and indirect, secondary interactions by means of proteoglycan aggregates.

Because collagen fibers have a degree of rigidity (and an associated persistence length), the effect of increasing n on the short-range order will saturate. In terms of a crosslink model, this is easily understood. As the crosslink density exceeds 1 over the persistence length, the effect of additional crosslinks will be minimal because the fibers are already fixed in space. Although the crosslink scenario is illustrative, this saturation feature is independent of the exact interaction mechanism. An additional feature of this relation must of course be that as n goes to 0 (i.e., no interactions), ξ must also go to 0. A sample function satisfying these qualitative features is given by

$$\xi = \xi_{max}\,(1 - e^{-n/n_0}) \tag{6}$$

There are numerous other functions that could satisfy the required features of $\xi(n)$, and this one was chosen only for its simplicity. In the simple crosslink model, the meaning of n_0 is clearly related to the inverse persistence length of the collagen fibers, whereas n can be thought of as a linear crosslink density.

The next step involves a qualitative study of the relation between collagen interaction and the aggregate modulus, i.e., the function $H(n)$. This relation is complex and incompletely understood. Here we are helped by the qualitative features of our data. To help elucidate our results, we need to understand only certain general features of this relation over a restricted range. In particular, for small n/n_0, the aggregate modulus can be expanded in a Taylor series:

$$H(n) \approx H_0 + H_1(n/n_0) + \ldots \tag{7}$$

The vertical asymptote demonstrated by the data corresponds to the limit of arbitrarily small n and the location of the asymptote to H_0. Likewise, the presence of the horizontal asymptote means that our choice of relation between H and n will not change the qualitative features of the horizontal asymptote or its location. The qualitative features of our results, including both asymptotes and their locations, can be explained with a Taylor expansion of H in terms of the collagen interaction parameter. The shortcoming of this approach is that it is not clear how well the central portion of the data, in the vicinity of the "elbow," are explained. It is important to note, as we will see below, that two of the fit parameters are indeed associated with the asymptotes.

The results of Eqs. 5-7 let us construct our semi-empirical expression for the dependence of average scatter angle on H, which is technically only valid near the asymptotes:

$$\langle\theta\rangle \approx \frac{\lambda\,\xi_{max}}{(1 - e^{(H_0 - H)/H_1})} \tag{8}$$

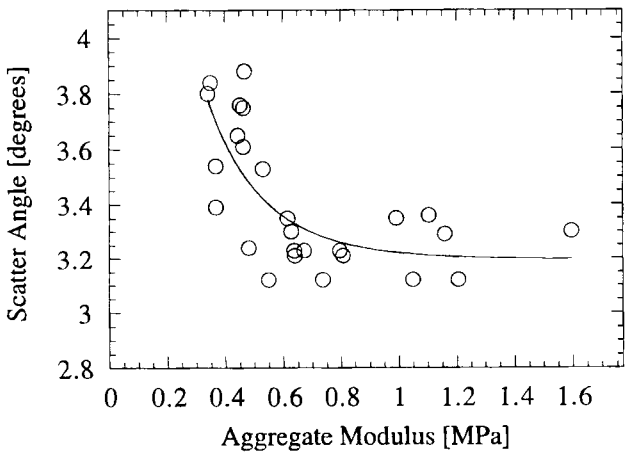

FIG. 3. Plot of average scatter angle, as defined by Eq. 1, relative to aggregate compressive modulus. The solid line represents the theoretical result, Eq. 8, using values for the fit parameters given in the text.

RESULTS

The average scatter angle had a pronounced dependence on the aggregate modulus (Fig. 3). This dependence was minimal at values greater than 0.6 MPa. There was an abrupt increase in scatter angle with decreasing modulus at values less than 0.6 MPa. The curve plotting scatter angle relative to aggregate modulus has a biasymptotic appearance in which the scatter angle approaches an asymptotic limit for large values of the modulus and the modulus approaches an asymptotic limit for larger scatter angles. This appearance is consistent with our theoretical model as described above and shown in Fig. 3.

The statistical significance of the relation between aggregate modulus and scatter angle can be expressed in terms of the R value of the fit of the theoretically determined expression, Eq. 8, that gives $R = 0.75$, with fit parameters H_0, H_1, and ξ_{max} of $H_0 = -0.075$ MPa, $H_1 = 0.22$ MPa, and $\xi_{max} = 8.2$ μm. The solid curve shown in Fig. 3 is a graph of Eq. 8 using these parameters. For a linear fit to the data, $R = 0.55$.

The relationships between permeability and aver-

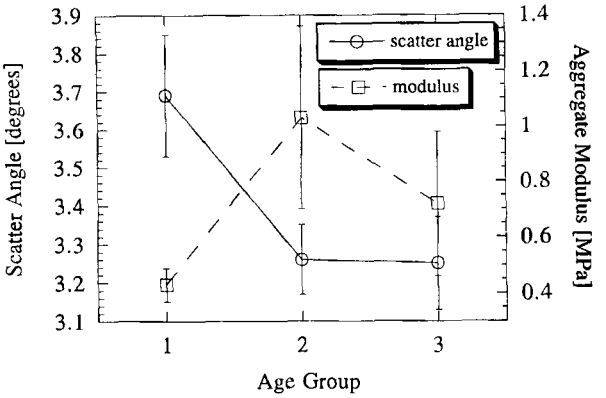

FIG. 4. Plot of average aggregate modulus and scatter angle relative to age group, with SDs. Group-1 animals were less than 3 years old (n = 9), group-2 animals were 3-10 years old (n = 6), and group-3 animals were more than 10 years old (n = 11).

age scatter angle and between Poisson's ratio and average scatter angle were also examined. A weak dependence of average scatter angle on permeability was noted (increasing permeability was associated with increasing average scatter angle), with a linear fit giving $R = 0.38$. A trend of decreasing scatter angle associated with increasing Poisson's ratio was also observed, with $R = 0.34$.

The relations between the specimen age and both the scatter and mechanical properties were also examined. It was found that the skeletally immature animals (n = nine test sites) and the skeletally mature animals (n = 17 test sites) differed in both their average aggregate modulus, 0.43 ± 0.06 MPa for the immature and 0.82 ± 0.31 MPa for the mature animals, and their average scatter angle, 3.63 ± 0.22° for the immature and 3.28 ± 0.17° for the mature animals. The statistical significance of these differences as calculated using the unpaired two-tailed t test was $p < 0.01$ for both the scatter angle and the modulus. No correlation was found between age and scatter angle or aggregate modulus once maturity had been reached (Fig. 4).

The relations between age and both scatter angle and permeability were also examined. A weak dependence of permeability on age was noted, with the immature animals having slightly more permeable cartilage than the mature animals ($1.84 \pm 0.92 \times 10^{-14}$ and $2.43 \pm 0.51 \times 10^{-14}$ m⁴/Nsec, respectively). This difference was, however, not statistically significant, with $p = 0.10$ using the unpaired two-tailed t test and $R = 0.41$ for a linear regression with age relative to permeability. There was no discernible dependence of Poisson's ratio on age or maturity, with $R = 0.14$ for a linear regression.

The effect of beam polarization angle, i.e., the orientation of the electric field vector in the laser light, with respect to the sample, was investigated by rotating the laser polarization and by rotating the sample around the beam axis. There was no discernible dependence of the scatter pattern on this parameter.

DISCUSSION

The results of this study demonstrate a clear relationship between the angular dependence of the intensity of light scattered from cartilage and its compressive mechanical properties. This should not come as a surprise given that both light-scattering characteristics and material properties should depend on small-scale structure. The light-scattering pattern from cartilage contains detailed information about the microarchitecture, notably the spatial arrangement of the collagen network. Likewise, the microarchitecture of cartilage should be intimately related to its mechanical properties. Although proteoglycan, not collagen, is typically associated with the compressive characteristics of cartilage, it is generally accepted that collagen plays an important role in determining the compressive properties of cartilage by opposing proteoglycan swelling, thereby influencing the degree of hydration (7,16).

In the analytical methodology section, a semiempirical theory is put forth to describe the observed relation between compressive modulus and average scatter angle in terms of spatial correlation of collagen fibers. A number of parameters in this theory are of potential physical significance. First, the location of the horizontal asymptote is just the inverse of the maximum degree of short-range order, i.e., the maximum distance over which collagen fibers influence the position of adjacent fibers. In our data, this maximum order parameter was determined to be about 8 μm. Another interesting parameter is the location of the vertical asymptote. H_0 corresponds to the component of the modulus that is independent of the collagen interactions. The location and convergence of the vertical axis may help clarify the role of collagen prestress and collagen fiber interaction in determining the compressive properties of intact cartilage.

It should be noted that the light-scattering data represent information obtained from the superficial zone of the cartilage, whereas the mechanical data are obtained from full-thickness specimens, and hence characteristics of all layers contributed to some extent. The superficial zone was chosen for the scattering experiments because it was felt, on the basis of existing finite element data (17), that the more superficial region would be of unequivocal importance in determining the mechanical properties. The deeper zones, while certainly a factor in determining the mechanical properties, are thought to contribute to a lesser degree to those properties observed at the surface.

There are several shortcomings in this experimental approach that require further experiments to clarify.

First, the angular dependence of the scatter is in fact the result of the product of the structure factor and the scatter pattern from individual fibers, as shown in Eq. 2. Thus, quantitative conclusions about the short-range order parameter are subject to a bias arising from the single fiber scatter factor. This is of potential significance in interpreting the results from immature animals, which may differ in terms of structure and arrangement of collagen fibers. Second, the fit values determined for H_0 and H_1 in the semi-empirical model are highly dependent on the structure of the function chosen for $\xi(n)$, the details of which are not known.

An additional caveat in the interpretation of these results in terms of collagen scattering lies in the possible role of proteoglycan scattering. A predominant role of collagen can be expected on the basis of the concentration of proteoglycan in cartilage, which is sufficiently high for it to constitute more of a continuum, with minimal refractive index variation at the optical wavelength scale, as opposed to discrete regions of refractive index change. Scattering from the structure within proteoglycan units (i.e., adjacent glycosaminoglycan chains) would not be expected to be significant due to the small-distance scales associated with these variations in refractive index (2). In addition, a predominance of collagen scatter has been noted in other tissues (2,8,15). Despite this, the results of this study do not preclude variations in the scatter arising in part from variations in aggrecan structure.

The future direction of this work lies to large extent in the study of larger angle scatter, selective degradation, the inclusion of strain effects in the scatter, and in the comparison with tensile mechanical properties. By going to larger angles, structure on a smaller scale, i.e., at the level of collagen fiber spacing, can be explored. By studying the effects of selective degradation and stress in conjunction with tensile characterization and larger angle scatter, a great deal of information relating microarchitecture to mechanical function may be unveiled. In addition, zonal variations in both the scatter properties and the mechanical properties could prove to be of interest and warrant further investigation.

To our knowledge, this work describes the first use of laser light-scattering techniques in the study of articular cartilage. It demonstrates a correlation between the small-angle light-scattering characteristics of articular cartilage and its compressive mechanical properties. A semi-empirical, theoretical explanation of this relation in terms of the degree of short-range order in the collagen network is presented that introduces a number of novel concepts into the description of the extracellular matrix in cartilage. The further application of optical methods in the study of cartilage may have far-reaching implications in helping to understand the mechanical function of cartilage in terms of its microscopic structure.

Acknowledgment: We would like to express our gratitude to Dr. Richards-Kortum for helpful discussions and use of the spectroscopy facilities at the University of Texas at Austin. We appreciate the technical assistance of David Stevens, Colin Smithpeter, and Andrew Dunn. The specimens were generously provided by The Southwest Foundation for Biomedical Research.

REFERENCES

1. Athanasiou KA, Agarwal A, Muffoletto A, Dzida FJ, Constantinides G, Clem M: Biomechanical properties of hip cartilage in experimental animal models. *Clin Orthop* 316:254-266, 1995
2. Benedek G: Theory of transparency of the eye. *Appl Optics* 10:459-473, 1971
3. Benedek G, Clark J, Serrallach E, Young C, Mengel L, Sauke T, Bagg A, Benedek K: Light scattering and reversible cataracts in calf and human lenses. *Philos Trans R Soc Lond* A293:329-340, 1979
4. Castanho MA, Brown W, Prieto MJ: Rod-like cholesterol micelles in aqueous solution studied using polarized and depolarized dynamic light scattering. *Biophys J* 63:1455-1461, 1992
5. Hunziker EB, Schenk RK: Structural organization of proteoglycans in cartilage. In: *Biology of Proteoglycans*, pp 155-183. Ed by TN Wight and RP Mecham. New York, Academic Press, 1988
6. Kerker M: *The Scattering of Light, and Other Electromagnetic Radiation*. New York, Academic Press, 1969
7. Kovach I: A molecular theory of cartilage viscoelasticity. *Biophys Chem* 59:61-73, 1996
8. Kronick P, Buechler P: Fiber orientation in calfskin by laser light scattering or x-ray diffraction and quantitative relation to mechanical properties. *J Am Leather Chem Assoc* 81:221-229, 1986
9. Mak AF, Lai WM, Mow VC: Biphasic indentation of articular cartilage. I. Theoretical analysis. *J Biomech* 20:703-714, 1987
10. Mecham RP, Heuser J: Three-dimensional organization of extracellular matrix in elastic cartilage as viewed by quick freeze, deep etch electron microscopy. *Connect Tissue Res* 24:83-93, 1990
11. Mow VC, Proctor CS, Kelly MA: Biomechanics of articular cartilage. In: *Basic Biomechanics of the Musculoskeletal System*, 2nd ed, pp 31-57. Ed by M Nordin and VH Frankel. Philadelphia, Lea & Febiger, 1989
12. Muir H, Bullough P, Maroudas A: The distribution of collagen in human articular cartilage with some of its physiologic implications. *J Bone Joint Surg [Br]* 52:554-563, 1970
13. Niederauer GG, Stevens DM, Athanasiou KA: Effects of aging on the mechanical properties in baboon knee cartilage. *Trans Orthop Res Soc* 21:265, 1996
14. Reihanian H, Jamieson AM, Tang LH, Rosenberg L: Hydrodynamic properties of proteoglycan subunit from bovine nasal cartilage: self-association behavior and interaction with hyaluronate studied by laser light scattering. *Biopolymers* 18:1727-1747, 1979
15. Sacks MS, Chuong CJ: Characterization of collagen fiber architecture in the canine diaphragmatic central tendon. *J Biomech Eng* 114:183-190, 1992
16. Schwartz MH, Leo PH, Lewis JL: A microstructural model for the elastic response of articular cartilage. *J Biomech* 27:865-873, 1994
17. Spilker RL, Suh JK, Mow VC: A finite element analysis of the indentation stress-relaxation response of linear biphasic articular cartilage. *J Biomech Eng* 114:191-201, 1992
18. Stein R, Erhardt P, van Artsen J, Clough S, Rhodes M: Theory of light scattering from oriented and fiber structures. *J Polym Sci* 13:1-35, 1966